Am J Transl Res 2019;11(6):3629-3636
www.ajtr.org /ISSN:1943-8141/AJTR0092638

Original Article

Influence of the plasminogen activator system on necrosis in acute myocardial infarction: analysis of urokinase- and urokinase receptor-knockout mouse models

Joerg Herold[1], Felix M Heidrich[3], Silvio Quick[3], Tobias Loehn[3], Karim Ibrahim[3], Adrian Mahlmann[2*], Akram Youssef[3*]

[1]Department of Vascular Medicine, Klinikum Darmstadt GmbH, Darmstadt, Germany; [2]University Centre for Vascular Medicine and Department of Medicine-Section Angiology, University Hospital Carl Gustav Carus at The Technische Universität Dresden, Germany; [3]Department for Internal Medicine and Cardiology, Herzzentrum Dresden, University Clinic, Technische Universität Dresden, Germany. [*]Equal contributors.

Received February 16, 2019; Accepted May 31, 2019; Epub June 15, 2019; Published June 30, 2019

Abstract: Serine proteases and G-protein-coupled receptors have been studied extensively as effectors of cell death. However, their roles in myocardial infarction have not been determined. In this study, we investigated the influence of the plasminogen activator system involving urokinase and urokinase receptor on necrosis after acute myocardial infarction. Myocardial infarction and reperfusion were induced in mouse hearts using the *in vitro* Langendorff model. DNA fragmentation and cleaved caspase-3 activity in urokinase- ($uPA^{-/-}$) and urokinase receptor-knockout mice ($uPAR^{-/-}$) were determined and compared with those in wild-type mice using *in situ* nick-end DNA labeling (TUNEL) and enzyme-linked immunosorbent assays, respectively. Infarct sizes were determined using propidium iodide and fluorescent microspheres. Following regional ischemia and reperfusion, a significant increase in the number of TUNEL-positive nuclei was observed in the ischemic zone in mouse hearts and to a lesser degree in regions remote from the ischemic area in wild-type, $uPAR^{-/-}$, and $uPA^{-/-}$ groups compared with those in directly removed hearts. No significant differences were observed between $uPAR^{-/-}$ and wild-type mice. Conversely, a significant reduction in DNA fragmentation was observed in ischemic and nonischemic regions after acute myocardial infarction in $uPA^{-/-}$ mice when compared with that in wild-type and $uPAR^{-/-}$ groups. The resulting infarct sizes were significantly smaller in $uPA^{-/-}$ mice than in $uPAR^{-/-}$ and wild-type mice. These data demonstrated the involvement of uPA, but not uPAR, in protecting against necrosis during acute myocardial infarction.

Keywords: Apoptosis, infarction, reperfusion, matrix metalloproteinases, transgenic animal models

Introduction

Cell death plays a central role in myocardial infarction, not only in the ischemic region but also in the nonischemic zone. We and others have shown in mice and rats that chronic infarction induced by ligating a coronary artery leads to increases in the number of terminal deoxynucleotidyl transferase dUTP nick end labeling (TUNEL)-positive cardiomyocytes, cleaved caspase-3 activity, and positive DNA laddering. These data suggest that apoptosis also occurs in the remote zone relative to the myocardial infarction [1-5]. Cell death after myocardial infarction is regarded as an important pathophysiological process leading to ventricular dysfunction and cardiac remodeling.

Attempts to inhibit key pro-apoptotic proteins, particularly caspase-3, have resulted in significant reductions in cardiomyocyte apoptosis and remodeling after chronic myocardial infarction [6, 7]. However, little is known regarding the specific pathogenic mechanisms and signal transduction in apoptosis that result in remodeling after myocardial infarction. The urokinase (uPA)-type plasminogen activator system and activation of serine proteases have been shown

to play important roles in ventricular and vascular remodeling [8]. uPA is a serine protease that functions in proteolysis during fibrinolysis and in the degradation of the extracellular matrix. Moreover, uPA also mediates signal transduction in cellular adhesion, differentiation, proliferation, and migration via interactions with the G-protein-coupled uPA receptor (uPAR) [9-12]. uPA has been shown to interact directly with vitronectin, caveolin, and integrins [13, 14]. Moreover, Gaertner et al. found that activation and upregulation of uPA occurred 3 months after regional myocardial infarction in rats. This increase was significantly higher in the ischemic region than in the nonischemic zone [15]. Furthermore, Knoepfler et al. found a four-fold increase in uPA activity in the ischemic zone in pig hearts [16]. In uPA-knockout ($uPA^{-/-}$) mice, no rupturing of the ischemic region after myocardial infarction occurred; moreover, significantly improved left ventricle function and reduced cardiac remodeling were observed when compared with that in controls at 7 weeks after aortic banding [17, 18]. These data suggest that the uPA system may be involved in the spreading of the infarcted zone and the remodeling process after coronary occlusion [19-23].

Accordingly, in this study, we investigated the influence of the uPA-type plasminogen activator system on cell death after acute myocardial infarction. We assessed this effect simultaneously in the ischemic and nonischemic zones in $uPAR^{-/-}$ and $uPA^{-/-}$ mouse models.

Materials and methods

Animals

Male 10-week-old C57BL6 mice (Charles River, Sulzfeld, Germany), with an average weight of 24.8 ± 2 g, were used as wild-type mice for comparison with the homozygous $uPAR^{-/-}$ and uPA^{-PA} mice (10-week-old males, average weight: $uPAR^{-uP}$, 22.4 ± 3 g; uPA^{-uP}, 21.1 ± 3 g). Knockout mice were also derived from a C57 strain. Our study adhered to the *Guide for the Care and Use of Laboratory Animals* published by the US National Institutes of Health (NIH Publication No. 85-23, revised 1996). The procedures for genotyping of transgenic animals are described in the Supplementary Material. All animal experiments were approved by our institutional animal care and use committee.

Langendorff isolated perfusion

Following intraperitoneal anesthesia with sodium thiopentone (Trapanal 25 mg/mL) in combination with heparin (10,000 IU/mL), the mouse thorax was opened, and the beating heart was dissected free from the aorta. The aortic root was connected to the Langendorff perfusion system, and Krebs-Henseleit solution was oxygenated using Carbogen (5% vol. CO_2, 95% vol. O_2; Linde, Germany) at a pH of 7.4 (38°C). A cardiac pacemaker stimulated the spontaneously beating heart at a fixed rate of 500 beats/min. After a 30-min perfusion period for equilibration, the left anterior descending artery (LAD) was encircled with a Perma-Hand silk suture (Ethicon 5.0; Norderstedt, Germany) distal to the circumflex branch. To induce ligation, an occluder was advanced over the ligature suture onto the coronary vessel and fixed with a clamp to maintain temporary regional ischemia for 60 min. The occluders were omitted in sham-operated controls. The 60-min regional ischemia was followed by reopening of the LAD and a 120-min period of reperfusion. Finally, the mouse hearts were embedded in tissue freezing medium (Leica Instruments, Nussloch, Germany) for TUNEL assays, frozen in liquid nitrogen, and stored at -80°C. For western blotting and enzyme-linked immunosorbent assay (ELISA), biopsies were collected at the end of the experiment from the central ischemic region and the nonischemic zone of the posterior wall, frozen in liquid nitrogen, and stored at -80°C. During LAD occlusion, the ischemic zone could be clearly identified as a pallor region in the myocardium.

TUNEL staining

To detect single- or double-strand DNA breaks, we used an *In-Situ* Cell-Death Detection Fluorescein Kit (Roche Diagnostics Applied Science, Mannheim, Germany). Five-micrometer-thick frozen heart sections were generated using a microtome (CM 1900; Leica). Cell nuclei were stained with 4',6-diamidino-2-phenylindoldihydrochloride (Invitrogen, Karlsruhe, Germany), and the slides were embedded in ProTaqs Mount Fluor (Biocyc, Luckenwalde, Germany) and analyzed using fluorescence microscopy (Roche). The ratio of the number of TUNEL-positive nuclei to the total number of nuclei was analyzed using MetaMorph software (Visitron

Systems, Puchheim, Germany) as described previously [24].

Western blotting

The biopsies were homogenized in 50-5-2-1 buffer (50 mM Tris HCl, 5 mM ethylenediaminetetraacetic acid, 2 mM ethylene glycol-bis[β-aminoethyl ether]-N,N,N',N'-tetraacetic acid, 1 mM phenylmethylsulfonyl fluoride, 1 mM benzamidine, pH 7.4, 4°C) with an Ultraturrax instrument (Jahnke & Kunkel IKA Labortechnik, Staufen, Germany). The homogenate was centrifuged for 10 min at 360 × *g* (4°C). Next, the supernatant was centrifuged for 20 min at 50,000 × *g* (4°C). The supernatant contained the soluble fraction, the pellet, and the particulate fraction. Western blotting was carried out using the Laemmli (14% sodium dodecyl sulfate polyacrylamide gels) and Towbin methods, followed by transfer to polyvinyl fluoride membranes as described previously [24]. Detection was performed using 1:1000 dilutions of primary anti-cleaved caspase-3 (Asp 175) antibodies (Cell Signaling Technology, Frankfurt, Germany) and secondary goat anti-rabbit antibodies (cat. no. sc-2054; Santa Cruz Biotechnology, Heidelberg, Germany), followed by development using an enhanced chemiluminescence kit (Amersham, Freiburg, Germany). Mouse NIH cells treated with staurosporine were used as positive control.

ELISA

To quantify the activity of cleaved caspase-3 in myocardial biopsies, we used an active caspase-3 ELISA kit (Merck Biosciences, Darmstadt, Germany). The myocardial tissue was first homogenized in lysis buffer with an Ultraturrax instrument and then incubated with a biotin-ZVKD-FMC inhibitor. Protein concentrations were determined using a bicinchoninic acid assay kit, and absorbance at 450 nm (two replicates) was measured using an ELISA plate reader (MWG Biotech, Ebersbach, Germany), with correction at 570 nm to rule out optical interference. The cleaved caspase-3 concentration was calculated from individual biopsies using a cleaved caspase-3 standard concentration series generated at the same time. After correcting the obtained cleaved caspase-3 values based on protein concentration, values were expressed as ng/mL/10 mg protein.

Determination of infarct size

Following the reperfusion period, 2 mL propidium iodide was inserted through the perfusion cannula when the LAD was opened. The LAD was then sealed by tightly tying the ligature threads, and 2 mL fluorescent microspheres was injected into the cannula. After storage at -80°C, three transverse heart sections of roughly equal thickness were cut distal to the ligature, starting from the apex. The cardiac sections were photographed in the dark under UV light, and the ratio of the infarcted zone to the risk zone was determined with ImageJ software [25].

Statistical analysis

SPSS software was used for data processing and analysis. The results are given as means ± standard errors of the means. For statistical calculations, analysis of variance was used with Sidak post-hoc testing. Results with *P* values of less than or equal to 0.05 were considered significant.

Results

DNA fragmentation developed after regional ischemia and reperfusion

Values obtained for hearts that were directly removed from wild-type, uPAR$^{-/-}$, and uPA$^{-/-}$ mice represented baseline values for comparison with those for hearts in the ischemia/reperfusion model (30-min equilibration, 60-min regional ischemia of the LAD, 120-min reperfusion). A perfusion control group was established using wild-type mice, which were subjected to the same steps excluding occlusion of the LAD and were perfused for a total of 3.5 h with Krebs-Henseleit solution using the Langendorff technique. This group was used to exclude the possible influence of a normoxic perfusion over the long period required for the *in vitro* perfusion and mechanical manipulations (owing to removal and suspension of the heart in the Langendorff device and encircling the LAD or cardiac pacemaker stimulation) when compared with that in hearts that were directly removed or hearts with regional ischemia and subsequent reperfusion.

In hearts that were directly removed, little DNA fragmentation, as indicated by TUNEL-positive

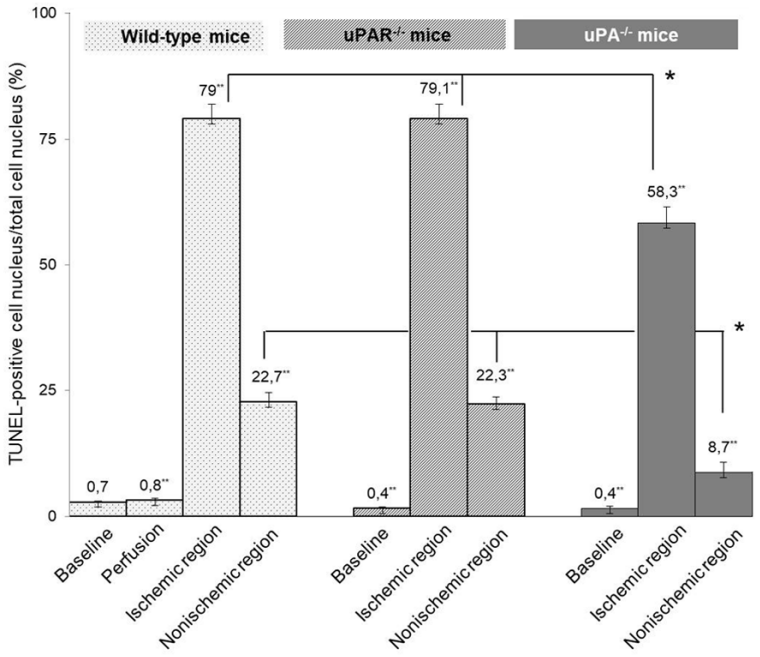

Figure 1. Changes in the number of TUNEL-positive nuclei. There were significant (*$P \leq 0.05$) increases in TUNEL-positive cell nuclei relative to the total number of nuclei after 60 min of regional ischemia followed by 120 min reperfusion in the ischemia region, albeit to a lesser extent in the nonischemic myocardium in wild-type, urokinase-knockout (uPA$^{-/-}$), and urokinase receptor-knockout (uPAR$^{-/-}$) mice compared with those in directly removed hearts (baseline) or the control group (perfusion). In the uPA$^{-/-}$ group, regional ischemia and reperfusion caused a significant reduction in the number of TUNEL-positive nuclei relative to the total number of nuclei when compared with those in wild-type and uPAR$^{-/-}$ mice.

nuclei, was found relative to the total number of nuclei (TUNEL indexes: wild-type, 0.7% ± 0.3%, n = 4; uPAR$^{-/-}$, 0.4% ± 0.2%, n = 4; uPA$^{-/-}$, 0.4% ± 0.4%, n = 4; **Figure 1**). In the control group including mouse hearts normoxically perfused for 3.5 h (n = 4), the TUNEL index was 0.8% ± 0.4%. No significant differences were observed between hearts that were directly removed and hearts after 3.5 h of normoxic perfusion. After 60 min of regional ischemia followed by a 120-min reperfusion period, there was a significant increase in the number of TUNEL-positive nuclei in the ischemic region distal to the temporarily occluded LAD in wild-type, uPAR$^{-/-}$, and uPA$^{-/-}$ mice (wild-type, 79.0% ± 2.9%, n = 4; uPAR$^{-/-}$, 79.1% ± 2.9%, n = 4; uPA$^{-/-}$, 58.3% ± 3.2%, n = 4; **Figure 1**). However, a significant increase in the number of TUNEL-positive nuclei was also observed in the remote, nonischemic myocardium when compared with baseline values in directly removed hearts (wild-type, 22.7% ± 2.0%, n = 4; uPAR$^{-/-}$, 22.3% ± 1.5%, n = 4; uPA$^{-/-}$, 8.7% ± 2.0%, n = 4; **Figure 1**). The TUNEL indexes for the ischemic region versus the nonischemic zone differed significantly between experimental groups (ischemic region versus nonischemic region: wild-type, uPAR$^{-/-}$, and uPA$^{-/-}$, $P \leq 0.05$). In the uPA$^{-/-}$ group, 60-min regional ischemia of the LAD followed by 120-min reperfusion caused a significant reduction in the number of TUNEL-positive nuclei relative to the total number of nuclei when compared with that in wild-type and uPAR$^{-/-}$ mice. This pattern was observed both in the ischemic zone and in the nonischemic region.

Cleaved caspase-3 expression after regional ischemia and reperfusion

Following regional ischemia and reperfusion in Langendorff-perfused mouse hearts in the wild-type, uPAR$^{-/-}$, and uPA$^{-/-}$ groups, the concentrations of active caspase-3 in biopsies from the ischemic and noninfarcted regions were measured by ELISA. The concentrations in the directly removed mouse hearts in the wild-type (12.9 ± 1.2 ng/mL/10 mg protein; n = 4), uPAR$^{-/-}$ (11.5 ± 1.8 ng/mL/10 mg protein; n = 4), and uPA$^{-/-}$ (10.9 ± 3.4 ng/mL/10 mg protein; n = 4) experimental groups were compared with those in control hearts after regional ischemia and reperfusion (**Figure 2**). A significant increase ($P \leq 0.05$) in the cleaved caspase-3 concentration was observed in the ischemic region and nonischemic zone compared with that in directly removed hearts (ischemic region versus non-ischemic zone: wild-type, 22.7 ± 2.7 versus 22.2 ± 3.2, n = 8; uPAR$^{-/-}$, 19.7 ± 3.0 versus 22.7 ± 3.6, n = 8; uPA$^{-/-}$ 24.2 ± 6.9 versus 22.7 ± 4.9 ng/mL/10 mg protein, n = 8). No significant differences ($P = 0.988$) were observed between the two myocardial regions.

Infarct size after regional ischemia and reperfusion

To quantify the extent of necrosis in the ischemic region, mouse hearts in the wild-type,

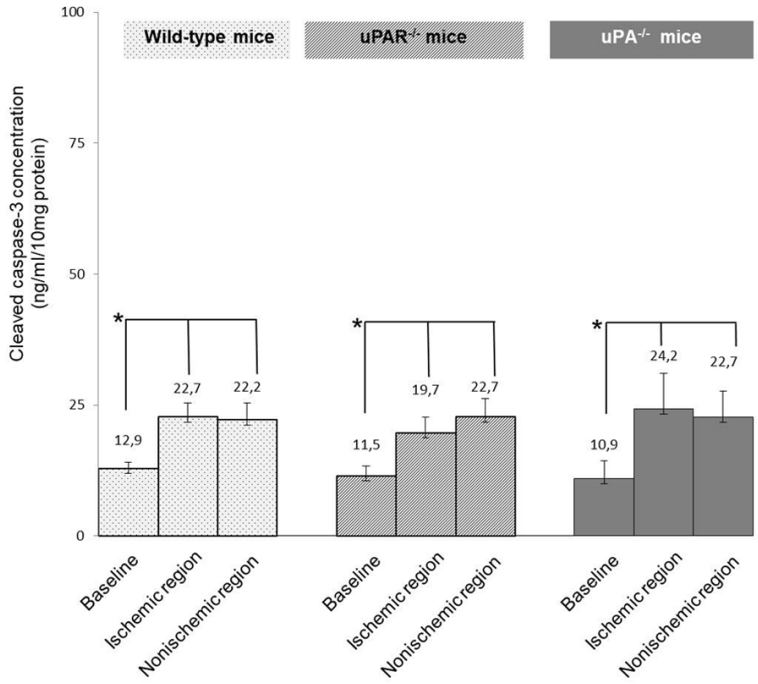

Figure 2. Changes in cleaved caspase-3 expression. Significant increases (*$P \leq 0.05$) in cleaved caspase-3 concentrations were detected by ELISA after regional ischemia (60 min) and reperfusion (120 min) in the ischemic and nonischemic myocardium of wild-type, uPAR$^{-/-}$, and uPA$^{-/-}$ mice compared with that in directly removed mouse hearts (baseline). No significant differences were observed between the ischemic and nonischemic regions ($p = 0.988$) or between different mouse groups ($P = 0.958$).

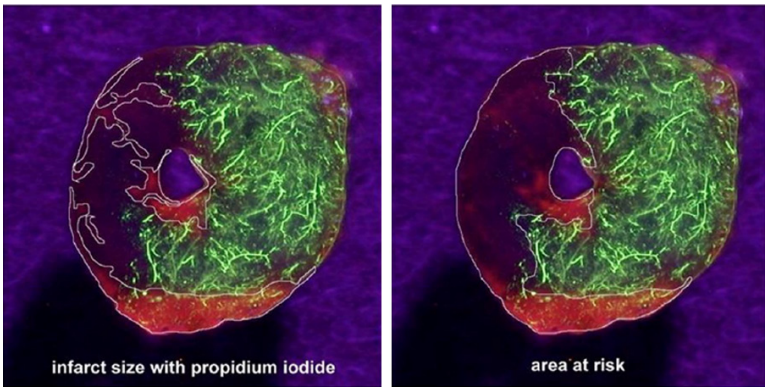

Figure 3. Quantification of the extent of necrosis. Necrosis was evaluated in the ischemic myocardium after regional ischemia and reperfusion following perfusion with propidium iodide at the end of the experiment. Counterstaining of the nonischemic region was performed with fluorescent microspheres (green) after ligation of the LAD. The infarcted areas with necrosis (blue) were related to the area at risk from the LAD (blue and red).

uPAR$^{-/-}$, and uPA$^{-/-}$ groups were perfused with propidium iodide at the end of the experiment, followed by counterstaining of the nonischemic zone with fluorescent microspheres after ligation of the LAD. The necrotic areas (infarct area) were related to the areas at risk from the LAD, and the infarct size was determined as a percentage of the total area (**Figure 3**). The infarct sizes following 60 min of regional ischemia and 120 min of reperfusion were 50.5% ± 9.0% in the wild-type group (n = 10), 49.7% ± 7.1% in the uPAR$^{-/-}$ group (n = 5), and 30.8% ± 5.0% in uPA$^{-/-}$ group (n = 5). Significantly smaller infarcts were observed in the uPA$^{-/-}$ group when compared with those in the wild-type and uPAR$^{-/-}$ groups ($P \leq 0.05$; **Figure 4**). No significant differences in infarct size were observed in wild-type and uPAR$^{-/-}$ mice ($P = 1.0$).

Discussion

In the current study, we observed marked DNA fragmentation after regional ischemia and reperfusion in the ischemic area and, to a lesser extent, in the nonischemic region; notably, uPAR$^{-/-}$ mice did not differ from wild-type mice. In contrast, uPA$^{-/-}$ mice show markedly lower DNA fragmentation both in the ischemic region and in the nonischemic zone. To the best of our knowledge, this is the first study to quantify the concentration of cleaved caspase-3 using ELISA in the two regions under investigation. However, the increase in cleaved caspase-3 concentrations owing to regional ischemia and reperfusion was low compared with the high DNA fragmentation observed by TUNEL staining. Moreover, in this model, there were no differences in cleaved caspase-3 concentrations between the ischemic region and the nonischemic zone. There were also no differences in cleaved caspase-3 concentrations

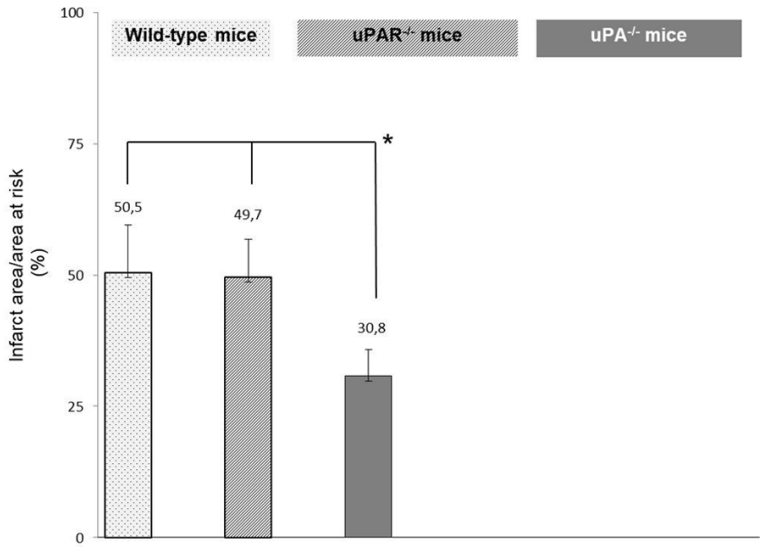

Figure 4. Infarct size. After regional ischemia (60 min) of the LAD and reperfusion (120 min), significantly smaller infarcts (infarct area/area at risk) were observed in the uPA$^{-/-}$ group when compared with those in the wild-type and uPAR$^{-/-}$ groups (*$P \leq 0.05$).

after regional ischemia and reperfusion among the wild-type, uPAR$^{-/-}$, and uPA$^{-/-}$ groups.

Consistent with the TUNEL results, uPA$^{-/-}$ mice show markedly smaller infarct sizes than wild-type and uPAR$^{-/-}$ mice. These data indicated that the absence of uPA exerted cardioprotective effects in acute myocardial infarction. Minatoguchi et al. demonstrated similar protective effects against myocardial infarction in a rabbit infarct model (30-min regional ischemia/48-h reperfusion) using a perfusion containing serine protease inhibitors, supporting the occurrence of caspase-independent reduction in DNA fragmentation after myocardial infarction [26].

DNA fragmentation in myocardial infarction is increasingly viewed as evidence of apoptosis or necrosis. Ohno et al. observed irreversible necrosis rather than apoptotic ultrastructures after ischemia and reperfusion (30-min regional ischemia/4-h reperfusion, in rabbits) in 83% of infarcted cardiomyocytes, despite positive TUNEL staining [27]. The timing and duration of ischemia and reperfusion are critical for the DNA fragmentation in myocardial infarction, considering the limitations of our *in vitro* model. Studies by Freude et al. showed that no TUNEL-positive DNA fragmentation occurred owing to ischemia alone in the absence of reperfusion (90-min global ischemia/6-h reperfusion, in a canine model). They found that the subsequent reperfusion was responsible for completion of the apoptotic cascade based on the functions of key pro-apoptotic proteins induced by ischemia. Moreover, Cheng et al. reported the occurrence of DNA fragmentation from 3 h to 1 month following coronary ligation [28]. Additionally, following ischemia, Freude et al. detected activated caspase-3 in 30% of cardiomyocytes and 90% of necrotic cardiomyocytes at the end of the reperfusion period [29]. McCully et al. described similar results, but found that necrosis was more prevalent than apoptosis (20-30-min global ischemia/2-h reperfusion, in rabbits) in the ischemic region [30]. Furthermore, after occlusion of a coronary artery, apoptosis occurs first, whereas necrosis is predominant later [31]. Attempts at inhibiting pro-apoptotic caspase-3 in myocardial infarction (30-min regional ischemia/6-h reperfusion, in rats) showed a reduction in DNA fragmentation without affecting the resulting infarct size [32]. Caspase-independent cell death has also been investigated in recent studies [33, 34], which have suggested a progression from apoptosis to necrosis [35]. In this study, only DNA fragmentation associated with high cleaved caspase-3 activity was defined as indicative of apoptosis. The high incidence of TUNEL-positive DNA fragmentation in relatively large infarcts and the concurrent low concentration of cleaved caspase-3 suggested the predominance of necrosis. uPA$^{-/-}$ mice showed lower DNA fragmentation and smaller infarct sizes after acute myocardial infarction, whereas uPAR$^{-/-}$ mice exhibited no significant differences when compared with wild-type mice. These findings suggested that in our model, uPA acted independently of the uPAR.

In summary, in this study, we demonstrated, for the first time, the effects of the uPA-type plasminogen activator system on the development of DNA fragmentation and infarct size in ischemic and nonischemic zones using a knockout

mouse model after acute myocardial infarction with regional ischemia and reperfusion. Our data suggested that this uPA system had protective effects against myocardial infarction, influencing infarct size and cell death. These protective effects did not appear to be mediated by the uPAR. However, our study was limited in that we did not perform histological, immunohistochemical, or gene expression analyses for mechanistic studies. Thus, further studies are needed to perform such analyses and to elucidate the signal transduction mechanisms underlying the observed protective effects of the uPA system. Indeed, the underlying mechanisms are still unknown. Cell-based models are needed in order to clarify the roles and interactions of uPA and uPAR in the myocardium.

Disclosure of conflict of interest

None.

Address correspondence to: Joerg Herold, Department of Vascular Medicine, Klinikum Darmstadt GmbH, Darmstadt, Germany. E-mail: joerg_herold@hotmail.com

References

[1] Abbate A, Bussani R, Biondi-Zoccai GG, Santini D, Petrolini A, De Giorgio F, Vasaturo F, Scarpa S, Severino A, Liuzzo G, Leone AM, Baldi F, Sinagra G, Silvestri F, Vetrovec GW, Crea F, Biasucci LM, Baldi A. Infarct-related artery occlusion, tissue markers of ischaemia, and increased apoptosis in the peri-infarct viable myocardium. Eur Heart J 2005; 26: 2039-2045.

[2] Biondi-Zoccai GG, Abbate A, Vasaturo F, Scarpa S, Santini D, Leone AM, Parisi Q, De Giorgio F, Bussani R, Silvestri F, Baldi F, Biasucci LM, Baldi A. Increased apoptosis in remote non-infarcted myocardium in multivessel coronary disease. Int J Cardiol 2004; 94: 105-110.

[3] Piro FR, di Gioia CR, Gallo P, Giordano C, d'Amati G. Is apoptosis a diagnostic marker of acute myocardial infarction? Arch Pathol Lab Med 2000; 124: 827-831.

[4] Sam F, Sawyer DB, Chang DL, Eberli FR, Ngoy S, Jain M, Amin J, Apstein CS, Colucci WS. Progressive left ventricular remodeling and apoptosis late after myocardial infarction in mouse heart. Am J Physiol Heart Circ Physiol 2000; 279: H422-428.

[5] Schwarz K, Simonis G, Yu X, Wiedemann S, Strasser RH. Apoptosis at a distance: remote activation of caspase-3 occurs early after myocardial infarction. Mol Cell Biochem 2006; 281: 45-54.

[6] Balsam LB, Kofidis T, Robbins RC. Caspase-3 inhibition preserves myocardial geometry and long-term function after infarction. J Surg Res 2005; 124: 194-200.

[7] Chandrashekhar Y, Sen S, Anway R, Shuros A, Anand I. Long-term caspase inhibition ameliorates apoptosis, reduces myocardial troponin-I cleavage, protects left ventricular function, and attenuates remodeling in rats with myocardial infarction. J Am Coll Cardiol 2004; 43: 295-301.

[8] Wu Q, Kuo HC, Deng GG. Serine proteases and cardiac function. Biochim Biophys Acta 2005; 1751: 82-94.

[9] Blasi F, Carmeliet P. uPAR: a versatile signalling orchestrator. Nat Rev Mol Cell Biol 2002; 3: 932-943.

[10] Ragno P. The urokinase receptor: a ligand or a receptor? Story of a sociable molecule. Cell Mol Life Sci 2006; 63: 1028-1037.

[11] Solberg H, Ploug M, Hoyer-Hansen G, Nielsen BS, Lund LR. The murine receptor for urokinase-type plasminogen activator is primarily expressed in tissues actively undergoing remodeling. J Histochem Cytochem 2001; 49: 237-246.

[12] Tkachuk V, Stepanova V, Little PJ, Bobik A. Regulation and role of urokinase plasminogen activator in vascular remodelling. Clin Exp Pharmacol Physiol 1996; 23: 759-765.

[13] Stahl A, Mueller BM. The urokinase-type plasminogen activator receptor, a GPI-linked protein, is localized in caveolae. J Cell Biol 1995; 129: 335-344.

[14] Franco P, Vocca I, Carriero MV, Alfano D, Cito L, Longanesi-Cattani I, Grieco P, Ossowski L, Stoppelli MP. Activation of urokinase receptor by a novel interaction between the connecting peptide region of urokinase and alpha v beta 5 integrin. J Cell Sci 2006; 119: 3424-3434.

[15] Gaertner R, Jacob MP, Prunier F, Angles-Cano E, Mercadier JJ, Michel JB. The plasminogen-MMP system is more activated in the scar than in viable myocardium 3 months post-MI in the rat. J Mol Cell Cardiol 2005; 38: 193-204.

[16] Knoepfler PS, Bloor CM, Carroll SM. Urokinase plasminogen activator activity is increased in the myocardium during coronary artery occlusion. J Mol Cell Cardiol 1995; 27: 1317-1324.

[17] Heymans S, Lupu F, Terclavers S, Vanwetswinkel B, Herbert JM, Baker A, Collen D, Carmeliet P, Moons L. Loss or inhibition of uPA or MMP-9 attenuates LV remodeling and dysfunction after acute pressure overload in mice. Am J Pathol 2005; 166: 15-25.

[18] Heymans S, Luttun A, Nuyens D, Theilmeier G, Creemers E, Moons L, Dyspersin GD, Cleutjens

JP, Shipley M, Angellilo A, Levi M, Nübe O, Baker A, Keshet E, Lupu F, Herbert JM, Smits JF, Shapiro SD, Baes M, Borgers M, Collen D, Daemen MJ, Carmeliet P. Inhibition of plasminogen activators or matrix metalloproteinases prevents cardiac rupture but impairs therapeutic angiogenesis and causes cardiac failure. Nat Med 1999; 5: 1135-1142.

[19] Adams JW, Brown JH. G-proteins in growth and apoptosis: lessons from the heart. Oncogene 2001; 20: 1626-1634.

[20] Alfano D, Franco P, Vocca I, Gambi N, Pisa V, Mancini A, Caputi M, Carriero MV, Iaccarino I, Stoppelli MP. The urokinase plasminogen activator and its receptor: role in cell growth and apoptosis. Thromb Haemost 2005; 93: 205-211.

[21] Barnes JA, Singh S, Gomes AV. Protease activated receptors in cardiovascular function and disease. Mol Cell Biochem 2004; 263: 227-239.

[22] Krishnamurthy P, Subramanian V, Singh M, Singh K. Deficiency of beta1 integrins results in increased myocardial dysfunction after myocardial infarction. Heart 2006; 92: 1309-1315.

[23] O'Mullane MJ, Baker MS. Elevated plasminogen receptor expression occurs as a degradative phase event in cellular apoptosis. Immunol Cell Biol 1999; 77: 249-255.

[24] Strasser RH, Simonis G, Schön SP, Braun MU, Ihl-Vahl R, Weinbrenner C, Marquetant R, Kübler W. Two distinct mechanisms mediate a differential regulation of protein kinase C isozymes in acute and prolonged myocardial ischemia. Circ Res 1999; 85: 77-87.

[25] Weinbrenner C, Schulze F, Sárváry L, Strasser RH. Remote preconditioning by infrarenal aortic occlusion is operative via delta1-opioid receptors and free radicals in vivo in the rat heart. Cardiovasc Res 2004; 61: 591-599.

[26] Minatoguchi S, Kariya T, Uno Y, Arai M, Nishida Y, Hashimoto K, Wang N, Aoyama T, Takemura G, Fujiwara T, Fujiwara H. Caspase-dependent and serine protease-dependent DNA fragmentation of myocytes in the ischemia-reperfused rabbit heart: these inhibitors do not reduce infarct size. Jpn Circ J 2001; 65: 907-911.

[27] Ohno M, Takemura G, Ohno A, Misao J, Hayakawa Y, Minatoguchi S, Fujiwara T, Fujiwara H. "Apoptotic" myocytes in infarct area in rabbit hearts may be oncotic myocytes with DNA fragmentation: analysis by immunogold electron microscopy combined with In situ nick end-labeling. Circulation 1998; 98: 1422-1430.

[28] Cheng W, Kajstura J, Nitahara JA, Li B, Reiss K, Liu Y, Clark WA, Krajewski S, Reed JC, Olivetti G, Anversa P. Programmed myocyte cell death affects the viable myocardium after infarction in rats. Exp Cell Res 1996; 226: 316-327.

[29] Freude B, Masters TN, Robicsek F, Fokin A, Kostin S, Zimmermann R, Ullmann C, Lorenz-Meyer S, Schaper J. Apoptosis is initiated by myocardial ischemia and executed during reperfusion. J Mol Cell Cardiol 2000; 32: 197-208.

[30] McCully JD, Wakiyama H, Hsieh YJ, Jones M, Levitsky S. Differential contribution of necrosis and apoptosis in myocardial ischemia-reperfusion injury. Am J Physiol Heart Circ Physiol 2004; 286: H1923-1935.

[31] Kajstura J, Cheng W, Reiss K, Clark WA, Sonnenblick EH, Krajewski S, Reed JC, Olivetti G, Anversa P. Apoptotic and necrotic myocyte cell deaths are independent contributing variables of infarct size in rats. Lab Invest 1996; 74: 86-107.

[32] Okamura T, Miura T, Takemura G, Fujiwara H, Iwamoto H, Kawamura S, Kimura M, Ikeda Y, Iwatate M, Matsuzaki M. Effect of caspase inhibitors on myocardial infarct size and myocyte DNA fragmentation in the ischemia-reperfused rat heart. Cardiovasc Res 2000; 45: 642-650.

[33] Johnson VL, Ko SC, Holmstrom TH, Eriksson JE, Chow SC. Effector caspases are dispensable for the early nuclear morphological changes during chemical-induced apoptosis. J Cell Sci 2000; 113: 2941-2953.

[34] Kroemer G, Martin SJ. Caspase-independent cell death. Nat Med 2005; 11: 725-730.

[35] Goldspink DF, Burniston JG, Ellison GM, Clark WA, Tan LB. Catecholamine-induced apoptosis and necrosis in cardiac and skeletal myocytes of the rat in vivo: the same or separate death pathways? Exp Physiol 2004; 89: 407-416.

Supplementary material

Methods

Genotyping of transgenic animals

DNA isolation: DNA isolation and purification from the tails of transgenic animals were performed using an Inivisorb Spin Tissue Mini Kit (Invitek, Berlin, Germany). The tissues were incubated with Proteinase K and Lysis Buffer G for 2 h at 52°C with continuous shaking. After centrifugation (2 min, maximum speed) to pellet the unlysed material, the supernatants were transferred to new tubes. After incubation with Binding Buffer T, the suspension was transferred onto a spin filter, incubated at 22°C for 1 min, and centrifuged for 2 min at 13,000 × g. The addition of the wash buffer onto the filter and the centrifugation step were performed twice (1 min at 13,000 × g; at the end of the washing procedure, the spin filter was centrifuged for 2 min at 13,000 × g). Following incubation, the spin filter was incubated with pre-warmed elution buffer D (at 52°C) for 3 min at room temperature, and genomic DNA was eluted by centrifugation for 2 min at 8,500 × g.

Polymerase chain reaction (PCR): Conventional PCR (Bio-Rad iCycler; Bio-Rad, Munich, Germany) was performed using specific primers (MWG, Ebersbach, Germany) to detect uPA$^{-/-}$ and uPAR$^{-/-}$ (94°C for 4 min; 40 cycles, 94°C for 30 s, 59°C for 30 s, 72°C for 30 s; 72°C for 4 min). The primer sequences were as follows: target allele for uPAR$^{-/-}$ mice (PCR product, 320 bp), uPAR KO (5'-TCATCAGTCCTC-CCTGCTAAGGGC-3') and HPRT#3 (5'-TATTACCAGTGAATCTTTGTCAGCAGTTCCC-3'); endogenous allele (uPAR$^{-/-}$ mice; PCR product, 147 bp), uPAR E3 3' (5'-CACCGGGTCTGGGCCTGTTGCAGAGGT-3') and uPAR E3 5' (5'-GATGATAGAGAGCTGGAGGTGGTGAC-3'); target allele for uPA$^{-/-}$ mice (PCR product, 200 bp), uPA B3 (5'-ATTGAATCCAGTCCAGGAAGTGTGAGACCC-3') and PGK P3'#2 (5'-CGCTACCGGTGGATGTGGAATG-TGT-3'); endogenous allele (uPA$^{-/-}$ mice; PCR product, 141 bp), uPA B1 (5'-GCGATTCTGGAGGACCGCTTAT-CT-3') and uPA B3 (5'-ATTGAATCCAGTCCAGGAAGTGTGAGACCC-3'). The resulting PCR products were loaded onto 1.6% agarose gels (with ethidium bromide) and run at 5 V/cm. Homozygous transgenic mice were identified by the simultaneous positive detection of the target allele and the absence of the endogenous allele (PCR product +320 bp/-147 bp in uPAR$^{-/-}$ +200 bp/-141 bp in uPA$^{-/-}$; Figure S1).

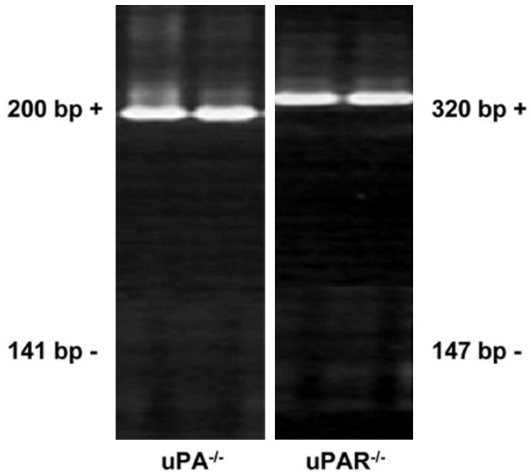

Figure S1. PCR products for urokinase knockout (+200 bp/-141 bp) and urokinase receptor knockout (+320 bp/-147 bp) mice.